Transposon-sequencing across multiple *Mycobacterium abscessus* isolates reveals significant functional genomic diversity among strains

Chidiebere Akusobi[1], Sanjeevani Choudhery[2], Bouchra S. Benghomari[3], Ian D. Wolf[1], Shreya Singhvi[4], Thomas R. Ioerger[2], Eric J. Rubin[1]

[1]Department of Immunology and Infectious Diseases, Harvard T.H. Chan School of Public Health, Boston, MA 02115, USA

[2]Department of Computer Science and Engineering, Texas A&M University, College Station, Texas 77843,

[3]Department of Biology, Northeastern University, Boston, MA 02115 USA

[4]Department of Molecular and Cell Biology, University of California, Berkeley, Berkeley, CA 94720 USA

Abstract

Mycobacterium abscessus (Mab) is a clinically significant pathogen and a highly genetically diverse species due to its large accessory genome. The functional consequence of this diversity remains unknown mainly because, to date, functional genomic studies in *Mab* have been primarily performed on reference strains. Given the growing public health threat of *Mab* infections, understanding the functional genomic differences among *Mab* clinical isolates can provide more insight into how its genetic diversity influences gene essentiality, clinically relevant phenotypes, and importantly, potential drug targets. To determine the functional genomic diversity among *Mab* strains, we conducted transposon-sequencing (TnSeq) on 21 genetically diverse clinical isolates, including 15 *M. abscessus subsp. abscessus* isolates and 6 *M. abscessus subsp. massiliense* isolates, cataloging all the essential and non-essential genes in each strain. Pan-genome analysis revealed a core set of 3845 genes and a large accessory genome of 11,507. We identified 259 core essential genes across the 21 clinical isolates and 425 differentially required genes, representing ~10% of the *Mab* core genome. We also identified genes whose requirements were sub-species, lineage, and isolate-specific. Finally, by correlating TnSeq profiles, we identified 19 previously uncharacterized genetic networks in *Mab*. Altogether, we find that *Mab* clinical isolates are not only genetically diverse but functionally diverse as well.

Introduction

Mycobacterium abscessus (Mab) has emerged in recent years as a growing threat to public health due to the rise of *Mab* infections worldwide (1). *Mab* causes a wide range of infections including 80% of pulmonary infections from rapidly growing mycobacteria (2,3). Treating *Mab* infections is difficult due to *Mab's* high level of intrinsic resistance to many antibiotics, including most of the cornerstones of tuberculosis treatment (4–7). Importantly, treating *Mab* requires identifying the subspecies of the clinical isolate, which influences antibiotic treatment based on the presence of *erm*, a gene that confers inducible macrolide resistance (8,9).

Mab is divided into three subspecies: *abscessus, bolletii,* and *massiliense* (10,11). Notably, most *massiliense* isolates lack an active *erm* gene (8,9). Whole-genome sequencing of *Mab* clinical isolates revealed that *Mab* has a large, open pan-genome, with isolates sharing ~75% of their genome in what is known as the 'core genome' (12,13). The remaining 25% of gene content is in the 'accessory genome' defined as genes present in some clinical isolates but not all. Most accessory genome content comprises plasmids, prophages, and genomic islands acquired by horizontal gene transfer (HGT) (14). Unlike *Mycobacterium tuberculosis (Mtb),* which evolves clonally likely due to its facultative intracellular lifestyle (15), the primary driver of *Mab* evolution is recombination and HGT (12,16,17). As a result, compared to TB, *Mab* clinical isolates have larger accessory genomes, which are significant contributors to the genetic diversity present in this species.

While *Mab* clinical isolates have large accessory genomes, the functional consequence of this diversity remains unknown. Previous studies have shown that accessory gene content impacts genetic networks, generating new phenotypes, gene dependencies, and redundancies within strains (18–20). Variation in accessory genomes likely generates functional genomic and phenotypic differences between isolates. The functional differences between isolates can be understood through genetic screens using CRISPRi and transposon-sequencing (TnSeq) libraries. TnSeq and the subsequent identification of essential genes have typically been conducted in lab-adapted reference strains. However, in recent years, groups have performed TnSeq on clinical isolates of pathogens, including *S. enterica, S. pneumoniae, S. aureus,* and

60 *M. tuberculosis.* These studies identified genes that were differentially essential among clinical isolates
61 and that these differences influenced clinically relevant phenotypes (19, 21–24).
62
63 For *Mab*, the majority of TnSeq studies published to date have used the lab-adapted reference strain,
64 ATCC 19977 (25–27). One TnSeq study was conducted on a *massiliense* clinical isolate; however, the
65 transposon library was not dense enough to quantify genetic requirement (28). Currently, there are no
66 published studies investigating the functional diversity of *Mab* clinical isolates. To accomplish this, we
67 conducted TnSeq on 21 *Mab* strains, generating triplicate libraries for 15 *abscessus* isolates and 6 single
68 libraries of the *massiliense* isolates. Across the 21 strains, we identified 425 genes, representing ~15% of
69 the *Mab* core genome, as differentially required among isolates. We also identified genes whose
70 differences in genetic requirements were sub-species, lineage, and isolate-specific. Finally, we identified
71 pairs of genes whose genetic requirements were correlated, revealing previously undescribed genetic
72 networks in *Mab*. Overall, we find that the genetic diversity in *Mab* clinical isolates is matched with
73 significant functional genomic diversity as well.

Results

Characterization of *Mab* clinical isolates

Our lab obtained 25 *Mab* clinical isolates previously collected from patients in Taiwan and locally at Brigham and Women's Hospital (BWH) (Supplemental Table 1). The clinical isolates represented a convenient sample of isolates to functionally characterize, given that they were isolated from multiple sites of infection, included both smooth and rough colony-morphology variants, and comprised both *abscessus* and *massiliense* subspecies. We passaged the clinical isolates only once to decrease selection of mutants under *in vitro* growth conditions. We then determined the genetic diversity of our clinical isolates through whole genome sequencing (WGS), followed by *de novo assembly* using ABySS (29) and annotation of the genomes using RAST (see Methods). The average number of nucleotides in the assemblies was 5103719 bp. Summary statistics of the WGS data are presented in Supplemental Table 2. A phylogeny of the 25 clinical isolates and five reference strains is shown in Figure 1A. The tree was generated using genome-wide SNP data while excluding SNPs from regions that showed evidence of a high degree of recombination, as determined by Gubbins (30). To put these isolates into a broader genomic context, they were incorporated into a global phylogeny constructed from 307 *Mab* isolates from Bryant *et al.* (11) using TNT (31). The resulting tree recapitulated the three subspecies of *Mab*, with our clinical isolates distributed across the entire tree (Figure 1B). About 60% of our isolates fell into clusters previously defined as dominant circulating clones (specifically *abscessus* DCC1 and *massiliense* DCC3) and are listed in Supplemental Table 1 (32).

Analysis of *Mab* core and accessory genome content

Next, we identified the clinical isolates' core and accessory genome content using the Ptolemy pan-genome analysis software program (33). From our panel of *Mab* clinical isolates, we identified 15,352 gene clusters representing distinct open reading frames (ORFs) (Supplemental Table 3). Of these, ~25% of the gene clusters were in the core genome, defined as present in at least 95% of the 30 isolates. The remaining ~75% of gene clusters, or 11,507 ORFs, were in the accessory genome (Figure 2A). The annotated genomes contained ~5200 genes, with accessory genes ranging from 997 to 1688. On average, the core genome comprised 75.6% of the total gene content in each strain, while the accessory

103 genome accounted for 24.4%. These values are consistent with results published from previous studies
104 (13,34). As expected, isolates more distantly related to the reference ATCC 19977 strain generally shared
105 less accessory genome content (Figure 2B). The diversity of the accessory genome was remarkable, as
106 evidenced by the number of isolates that contained distinct ORFs not present in any other isolates (Figure
107 2C). Of the 11,507 accessory genes identified, nearly 64% (n = 7361) were present in only one strain.
108 The remaining 4147 genes were present in multiple (2-28) isolates. Of these, 1114 were monophyletic
109 genes, meaning they were either inserted or deleted at one evolutionary time point and subsequently
110 inherited by all the strains on that branch of the phylogenetic tree. The remaining 3210 accessory genes
111 were polyphyletic. A subset of the monophyletic genes was sub-species specific and present in only
112 *abscessus, massiliense,* or *boletti* isolates (Figure 2D).
113
114 **Transposon-sequencing of multiple *Mab* clinical isolates**
115 Given the large genomic diversity present in *Mab*, we performed TnSeq across multiple clinical isolates to
116 characterize the species' functional diversity. The goal was to identify genes that were differentially
117 required among the isolates to better understand the functional diversity in *Mab.* Specifically, we sought
118 to identify a core set of essential genes in *Mab* clinical isolates and genes whose essentiality was sub-
119 species or lineage-specific. To do this, we selected 21 isolates for TnSeq, which spanned the
120 phylogenetic tree of *Mab*, including 15 *subsp. abscessus* and 6 *subsp. massiliense.* We then generated
121 libraries in triplicate for the *abscessus* subsp. isolates, and single replicate libraries for the *massiliense*
122 subsp. isolates. A schematic of the TnSeq experiment is presented in Supplemental Figure 1A. The
123 transduction efficiency of the clinical isolates varied greatly, with the highest efficiencies observed in the
124 two reference strains: ATCC 19977 and *massiliense* CCUG 48898 (hereafter referred to as *massiliense*)
125 (Supplemental Figure 1B). After transduction, >150,000 independent mutants were harvested from each
126 replicate, and sequencing libraries were prepared for next-generation sequencing. Of note, *subsp. bolletii*
127 libraries were not generated in this study due to the absence of clinical isolates in the lab.
128
129 Sequencing revealed that nearly all the transposon libraries were well-saturated, with a median saturation
130 of 59.5% ('TA' dinucleotide sites containing a transposon insertion). This range of saturation spanned

131 20% to 70.3% (Supplemental Figure 1C). Libraries with less than 33% saturation were excluded from
132 further analysis. Previous TnSeq studies demonstrated that downstream analyses of gene essentiality
133 performed well on libraries with saturation between 30%-80%. This analysis is also supported by the
134 sensitivity analyses for HMM, resampling, and ANOVA presented in the Supplemental Materials. The
135 summary statistics for each library are presented in Supplemental Table 4. To assess the reproducibility
136 of our replicates, we compared the mean number of insertions in each gene between pairs of replicate
137 libraries for each strain. We found that most replicates were well correlated with a median Pearson r^2
138 value of 0.88 (Supplemental Table 5).
139
140 **HMM reveals essential genes in *Mab* clinical isolates**
141 Using the Hidden Markov Model (HMM) algorithm (35), we determined the essentiality of genes in each
142 isolate. The genes were categorized as essential, non-essential, growth defect, or growth advantage.
143 Essential genes have no insertions in all or most of their TA sites. Genes classified as 'growth defect' are
144 not essential, but their disruption causes growth impairment, resulting in suppressed transposon insertion
145 counts. Conversely, when disrupted, genes classified as 'growth advantage' cause a fitness benefit
146 relative to wild type, resulting in increased insertion counts. The essential genes of the reference strain,
147 ATCC 19977, have been previously reported (25,27). We compared our predicted essential or growth-
148 defect genes for ATCC 19977 to those in Rifat *et al.* (25) and found an overlap of 393 genes, showing
149 high concordance between these two studies of *Mab* essentials (Supplemental Figure 2A). We also
150 compared our predicted *Mab* essentials and growth-defect genes with those from the related
151 mycobacterium *M. tuberculosis* (*Mtb* strain H37Rv) (36). There were 403 essential genes in common
152 among 2278 genes with mutual orthologs, demonstrating substantial conservation between the two
153 mycobacterial species (Supplemental Table 6). In total, there were 353 essential genes in the intersection
154 of all 3 datasets (Supplemental Figure 2A). These genes were significantly enriched in key cellular
155 pathways such as protein translation, amino acid metabolism, nucleotide metabolism, cell-cycle control,
156 and cell wall synthesis (Supplemental Figure 2B). We then used the HMM to determine essential genes
157 in all the clinical isolates. The essentiality call for each gene is listed in Supplemental Table 7. The
158 average number of essential (ES) genes across the clinical isolates was 345, with a range of 281–391.

159 The combined number of essential and growth-defect (ES+GD) genes (avg ~423) is consistent with
160 essentiality analyses of other mycobacteria, where essential genes typically represent 10-15% of the
161 genome (27). There were 259 pan-essential genes that were ES or GD across all 21 Mab isolates. These
162 genes are listed in Supplemental Table 7. Chi-squared analysis was used to identify 17 clade-specific
163 essential genes (Supplemental Figure 4), such as *mqo* (MAB_3159c, malate:quinone oxidoreductase),
164 which is only essential in subsp. *massiliense*.
165
166 **ANOVA identifies additional differentially required genes**
167 Next, we identified differentially required genes, defined as genes whose disruption causes varying
168 degrees of growth defect in isolates. Traditionally, the 'resampling' method from TRANSIT is used to
169 identify differentially required genes between two strains (35). We performed resampling between each
170 clinical isolate and the reference ATCC 19977 strain, and the conditionally essential genes are listed in
171 Supplemental Table 8. Resampling between pairs of isolates showed greater similarity (fewer
172 conditionally essential genes) in comparisons within the same subspecies than those between
173 subspecies (Supplemental Figure 5). These results gave us further confidence that our libraries were of
174 sufficient quality for further analyses.
175
176 To compare the transposon insertion counts across all strains simultaneously, we used ANOVA, which
177 identified 425 genes in the pan-genome (with adjusted P-value<0.05) that were differentially required
178 across all 21 clinical isolates (Supplemental Table 9). For each gene, the log2-fold-change (LFC) of the
179 insertion counts in each isolate was calculated relative to the grand mean across all isolates. These LFCs
180 are depicted in a heatmap (Figure 3). Hierarchical clustering of the isolates revealed that the *massiliense*
181 isolates (T36, T49, T52, BWH-D, BWH-F, massiliense) and the *abscessus* subspecies group together
182 (Figure 3). Thus, the phylogenetic tree generated from TnSeq data roughly recapitulates the phylogeny
183 generated from SNP differences (Figure 1A). The 425 differentially required genes represent 11% of the
184 *Mab* core genome. Furthermore, 337 of these genes are non-essential in the reference ATCC 19977
185 genome (Figure 3B). These data reinforce the concept that genes can be differentially required based on
186 genetic background (24).

187

188 **Gene essentiality varies by lineage and strain**

189 To better understand the variance in the ANOVA data set, we used principal component analysis (PCA)
190 to group the significant genes. The analysis showed principal components (PC) 1 & 2 explain ~40% of the
191 variation in the data (Figure 4A). When the isolates are clustered into three groups, they do so primarily
192 by phylogenetic relationship, where cluster 1 is a sub-lineage of the *abscessus* subspecies, cluster 2 has
193 the *abscessus* subspecies that are more closely related to the reference ATCC 19977 strain, and cluster
194 3 contains the *massiliense* subspecies. PCs 1 and 2 represent lineage-specific differences in gene
195 requirement, while when PCs 3 and 4 are plotted, the phylogenetic clustering collapses (Figure 4B). The
196 *Mab* phylogenetic tree is color-coded with the three corresponding clusters (Figure 4C). This analysis
197 demonstrates that closely related isolates share genetic requirements and suggests a shared
198 evolutionary origin of how these requirements arose.

199

200 The variation in PCs 1 and 2 only explains ~40% of the variation in the dataset, corresponding to lineage-
201 specific variation. In contrast, PCs 3-19 explain the remaining ~60% of the variation and likely represent
202 strain-specific variation or noise (Figure 4D). The top 10 genes contributing to the variance in PCs 1 and
203 2 are plotted in Figure 4E. The genes in PC 1 separate the two subspecies, while those in PC 2 separate
204 Cluster 1 strains (T35, T37, T50, and T56) from the rest of the clinical isolates (Figure 4E).

205

206 **Identification of genes with lineage-specific essentiality**

207 Next, we examined genes that exhibited lineage-specific differences in genetic requirement. We first
208 identified genes that separated the reference strain from the clinical isolates. Two genes were the
209 strongest differentiators: *MAB_4502c*, which encodes phosphoenolpyruvate carboxykinase (*pckA*), and
210 *MAB_1327,* which encodes ferredoxin *(fdxC*) (Figure 5A). The reference strain requires *pckA* less than
211 the clinical isolates, a difference that could be explained by laboratory adaptation of the reference strain.

212

213 Next, we analyzed the contributing genes in PC 1 that separate the two subspecies of *Mab abscessus* vs.
214 *massiliense.* The top 4 genes are depicted in Figure 5B, while the top 20 genes that separate the

215 subspecies are listed in Supplemental Table 10. We next inspected genes that separated strains in
216 Cluster 1 (T35, T37, T50, and T56) from the rest of the clinical isolates (Figure 5C). The top 20 genes
217 contributing to the variation in this cluster are listed in Supplemental Table 11.
218
219 The genes uniquely required in Cluster 1 can be split into three groups depending on how many strains
220 share the level of gene requirement. For group 1, all four strains in the cluster share the same
221 requirement for three genes in an operon, *MAB_2724c-MAB_2726c* (hypothetical genes of unknown
222 function). Group 2 genes are shared only by T35, T37, and T56, which are more related to each other
223 than T50. Finally, group 3 comprises genes shared by the two most closely related strains, T35 and T56.
224 These data reveal genetic requirements emerging within a lineage. As strains diverge, their genomes
225 change in genetic sequence and function, and genes that are otherwise dispensable in one strain can
226 become more required in another. This is best illustrated by genes *MAB_4950c* and *MAB_1055c*, which
227 are most strongly required in the two phylogenetically related isolates, T35 and T56 (Figure 5C).
228
229 **Correlated transposon insertion counts reveal functional genetic networks**
230 To extract functional inferences from our TnSeq dataset, we looked for pairs of genes with correlated
231 transposon insertion counts, which could reveal hidden functional genetic networks. To conduct this
232 analysis, we selected the 751 unique ORFs with the most variability based on ANOVA (p-adj < 0.05) and
233 other filters (see Methods). Of the 282,000 potential gene pairings, only 10,198 were significantly
234 correlated, representing 3.6% of total potential pairs (Supplemental Table 12). In Figure 6A, we show
235 three examples of gene pairs that are positively correlated. Pair 1 is genes *MAB_2725c x MAB_2726c*,
236 whose insertion counts were correlated with an r^2 of 0.92. The following two pairs, *MAB_2725c x*
237 *MAB_3333* and *MAB_3246c x MAB_3333,* also have statistically significant correlated insertion counts.
238 All these genes are correlated with each other and ostensibly form a network.
239
240 Based on these pairwise gene correlations, we performed network analysis with Cytoscape to turn these
241 pairwise correlations into a network of interconnected genes. The network was organized into 19 clusters
242 based on a greedy community identification algorithm (see Methods), so related genes with similar

243 transposon insertion profiles were clustered. This analysis identified 19 clusters containing at least five
244 genes (Supplemental Table 13). The genes profiled in Figure 6A are members of cluster 7 and are
245 starred in the network (Figure 6B). Cluster 7 is comprised of 13 genes and includes the previously
246 highlighted operon *MAB_2724c – MAB_2726* as well as 10 other genes, including *ruvA* and *ruvB*, which
247 both encode Holliday junction ATP-dependent DNA helicases, and *MAB_3246c*, which encodes *smc*,
248 segregation and condensation protein (Figure 6B). The complete network analysis with a few of the
249 clusters highlighted is depicted in Figure 6C. Importantly, only comparative analysis of TnSeq data could
250 reveal these genetic networks across multiple genetically diverse strains.
251
252 **Genes involved in central carbon metabolism are differentially required among clinical isolates**
253 Resampling analysis unveiled several differentially required genes involved in carbon metabolism among
254 the clinical isolates compared to the reference strain (Figure 7A). As noted above, *pckA* is more required
255 in clinical isolates than ATCC 19977. Other examples include *mqo* (malate:quinone oxidoreductase),
256 which is most required in T50 and BWH-F, and *pgi* (glucose-6-phosphate isomerase), which is most
257 required in T35 and T56. To validate these differences, we employed CRISPRi/Cas9 to repress *pckA*,
258 which is more required in nearly all the clinical isolates and is dispensable in ATCC 19977. We found that
259 when *pckA* is repressed in ATCC 19977, there was no difference in CFUs between induction and non-
260 induction plates as predicted by the TnSeq data (Figure 7B). However, when we repressed the enzyme in
261 T35 and T45, we observed a 10X to 100X decrease in CFUs, indicating that *pckA* is more required in
262 these clinical isolates. Notably, *pckA* was significantly more repressed in the reference strain than in the
263 clinical isolates (Supplemental Figure 6A). The lack of reduction in CFUs in the reference strain despite
264 stronger knockdown further supports *pckA's* dispensability in ATCC 19977 relative to the tested clinical
265 isolates.
266
267 We also repressed *sdhB*, which was predicted to be required in ATCC 19977 and less required in the
268 T49. Repressing *sdhB* in ATCC 19977 led to a 100X fold decrease in CFUs. However, when *sdhB* was
269 repressed in T49, there was no difference in CFUs, confirming that *sdhB* is less required in T49 (Figure
270 7B). These differences in CFUs were observed with similar levels of *sdhB* knockdown (Supplemental

271 Figure 6B). Altogether, these knockdown experiments validate our genetic requirement data and

272 corroborate the functional differences in carbon metabolism between the clinical isolates.

273 **Discussion**

274 While several groups have described the genomic diversity of *Mab* clinical isolates (13,16,17), to date, no
275 studies have interrogated the functional consequence of this diversity. To investigate the functional
276 diversity and genetic requirements of *Mab*, we performed TnSeq on 21 *Mab* clinical isolates spanning
277 both the *abscessus* and *massiliense* sub-species. Among the 21 isolates, we identified 425 genes, or
278 ~11% of the *Mab* core genome as being differentially required among the isolates. This includes non-
279 essential genes in the reference strain that became either fully essential or more required in some clinical
280 isolates.

281

282 Applying TnSeq to a genetically diverse group of isolates enabled us to uncover functional differences
283 among core and accessory genes. Using PCA and network analysis, we identified significant clusters of
284 genes whose insertion patterns were correlated and whose functional requirements varied with
285 phylogenetic position, either subspecies or lineage-specific. This data implied that *Mab* isolates have
286 evolved to require a distinct subset of genes. Given that our genetic screen was conducted under *in vitro*
287 conditions, passaging our transposon mutant libraries through more environmental or disease-relevant
288 conditions would reveal additional variability in genetic requirement. Recently, Sullivan *et al.* passaged a
289 transposon mutant library of clinical isolate T35 on an *in vitro* lung model and identified key genes
290 responsible for establishing lung infection (37).

291

292 We also identified differences in gene requirement that were lineage-specific. Strains T35, T37, T50, and
293 T56 represent one distinct lineage of the *abscessus* sub-species with genetic requirements unique to
294 these strains. Notably, the operon *MAB_2724c-MAB_2726c* was uniquely required in this lineage and
295 contributed 20% of the variance separating this sub-lineage from all the other clinical isolates. All three
296 genes in the operon are annotated as hypothetical proteins (orthologous to Rv1479-81 in *Mtb*), and future
297 studies are needed to understand why this operon is uniquely required in this subset of strains.

298

299 Interestingly, our study identified functional differences between the reference strain and the clinical
300 isolates in genes related to carbon metabolism. Specifically, the gene *MAB_4502c* encodes the enzyme

301 phosphoenolpyruvate carboxykinase, *pckA*, and is more required in nearly clinical isolates than the
302 reference strain. *pckA* catalyzes the conversion of oxaloacetate to phosphoenolpyruvate, the first
303 committed step of gluconeogenesis. The reduced requirement for *pckA* in ATCC 19977 is likely a
304 consequence of the reference strain passaged on rich media and adapting to ample carbon sources for
305 70+ years (38).
306
307 This study raises an open question: what role does the accessory genome play in driving variability in
308 genetic requirements among *Mab* strains? *Mab* is well-known to have a large accessory genome, which
309 we confirmed using pan-genome analysis. Gene acquisition and gene loss through plasmid transfer,
310 phage integration, duplication, or large-scale deletion likely influences genetic requirement and functional
311 differences between strains. More work is needed to untangle the effects of these accessory genes'
312 presence and absence on the core genome's essentiality. Nevertheless, this TnSeq dataset offers
313 valuable insight into variable functionality among *Mab* strains and provides a foundation for future study of
314 the biological and clinical consequences of genetic diversity of *Mab* clinical isolates.

315 **Methods**
316
317 **Bacterial strains and culture conditions:** *Mab* clinical strains were isolated from patients in Taiwan (T)
318 and Brigham and Women's Hospital (BWH), Boston, MA. Clinical isolates were streaked from patient
319 stabs; single colonies were picked, cultured, and frozen for future use. Strains with transformed
320 CRISPRi/Cas9 vectors to knockdown central carbon metabolism genes were built as described in (27). All
321 strains were grown shaking at 37°C in liquid 7H9 media consisting of Middlebrook 7H9 salts with 0.2%
322 glycerol, 0.85 g/L NaCl, and OADC (oleic acid, 5 g/L albumin, 2 g/L dextrose, 0.003 g/L catalase), and
323 0.05% Tween80. All *Mab* strains were plated on Middlebrook 7H10 agar supplemented with 10% OADC
324 and 0.05% Tween80. Kanamycin 100 µg/ml was used for selection. All CRISPRi/Cas9 plasmids were
325 induced with 500 ng/µl ATc.
326
327 **Whole Genome Sequencing of *Mab* Clinical Isolates:** Genomic DNA from late-log phase cultures were
328 extracted via a bead-beating and phenol-chloroform protocol described in Akusobi *et al.* (27), using an
329 Illumina Rapid HiSeq 2500 instrument with 125+125 bp paired-end reads.
330
331 **Genome Assembly:** Genome sequences for each isolate were assembled *de novo* from .fastq files using
332 ABySS (v2.0) with default parameters (29). The assemblies had a mean total length of 5.14 Mbp (range:
333 4.86-5.54 Mbp) (Supplemental Table 2). To assemble core genomes, the contigs were mapped onto the
334 *M. abscessus* ATCC 19977 (NC_010397.1) reference genome using Blastn and concatenated in syntenic
335 order. The final genome length and depth of coverage are shown in Supplemental Table 2. To distinguish
336 among *Mab* subspecies, the pattern of nucleotide substitutions was examined in *hsp65/groEL2* and rRNA
337 (internal-spacer) loci (39).
338
339 **Genome Alignment and Annotation:** Genome alignments were made using MUMMER v3.23 (40). To
340 identify SNPs and indels, regions with genetic variation were aligned using the Needleman-Wunsch
341 algorithm (41). For core genomes, the coordinates of open reading frames (ORFs) were adjusted for each
342 isolate using a whole-genome alignment to the reference genome. Genes whose start or end coordinates
343 were deleted in a clinical isolate were removed from the annotation. To produce unbiased annotations of

344 each clinical isolate, we ran RAST (PATRIC CLI v1.039) on the contigs generated by ABySS (42). These
345 annotations contain all predicted ORFs on all contigs.
346
347 **Phylogenetic Analysis:** An alignment of all the core genomes was first generated to construct a
348 phylogenetic tree incorporating all the *Mab* clinical isolates and reference strains. The included reference
349 strains are listed in Supplemental Table 2, with sequencing data for *M. abscessus* str. K21 kindly
350 provided by M. Gengenbacher. For all isolates, regions with insertions or deletions were filtered out, along
351 with sites exhibiting low coverage (<10x), heterogeneity (<70% base-call purity), or repetition (where an
352 overlapping window of 35 bp matches with at least 33/35 bp elsewhere in the genome). Finally, the
353 remaining list of SNPs was extracted and used as input to RAxML (43) to generate the maximum
354 likelihood phylogenetic tree, rooted using *M. bolletii* str. FLAC003 as an outgroup. Gubbins (30) was used
355 to identify and filter out genomic regions (at least 500 SNPs) potentially affected by recombination,
356 totaling <15% of the genome.
357
358 **Pan-Genome Analysis:** The pan-genome analysis was performed on 30 Mab strains (25 clinical isolates
359 and 5 reference strains) using Ptolemy v1.0 (33) to determine mappings of orthologs among ORFs based
360 on homology and synteny. ABySS assemblies were input for each isolate and the ORFs from the RAST
361 annotation. The output was used to generate a spreadsheet with all "pan-ORFs" (15,352 ortholog
362 clusters) as rows and individual ORF IDs in columns. This data is provided in Supplemental Table 3,
363 which also contains a count of how many of the 30 strains had a copy of each pan-ORF, which was used
364 to differentiate core genes (genes with orthologs in >95% of isolates) from accessory genes (present in 1-
365 28 isolates).
366
367 **Generation of Transposon Libraries:** High-density transposon libraries of selected *Mab* clinical isolates
368 were generated using the ϕMycoMarT7 phage described in Akusobi *et al.* (25–27). Libraries were
369 generated in biological triplicate for 15 clinical isolates, while single replicate libraries were generated for
370 6 isolates (see Supplemental Table 4). K21 was a generous gift from Thomas Dick, Meridian Health,
371 Hackensack, NJ.

372

373 Libraries were selected for 4 days on 7H10 agar supplemented with 10% OADC, 0.5% glycerol, 0.05%
374 Tween80, and 100 µg/ml kanamycin. Libraries of >150,000 mutants were harvested and stored in 7H9 +
375 10% glycerol at -80°C for future use. Transposon-sequencing libraries were prepared following the
376 protocol described in (44). The TnSeq samples were sequenced on an Illumina Rapid HiSeq 2500
377 instrument with 125+125 bp paired-end reads.

378

379 **TnSeq Analysis:** The .fastq files obtained from sequencing were pre-processed using TPP in Transit
380 (35). The reads were then mapped to the syntenic versions of each genome (aligned to ATCC 19977)
381 and the raw Abyss assemblies (all contigs) of each isolate. The median library saturation was 58.4%
382 (19.0-72.6%) (Supplemental Table 4). BWH-B-2, BWH-C-1, and all T44 strains were excluded from
383 further analyses due to low saturation or total insertion count.

384

385 The Hidden Markov Model (HMM) in Transit was run to identify essential and non-essential genes in each
386 isolate (Supplemental Table 7). Furthermore, the genes were evaluated by a confidence score based on
387 the consistency of the insertion statistics with the posterior distribution of the called essentiality state (see
388 Supplemental Material). Low-confidence genes (<0.20) were filtered out of the analyses. The 'resampling'
389 method in Transit was used to identify conditionally essential genes in each isolate relative to ATCC
390 19977. p-values were adjusted for multiple tests using the Benjamini-Hochberg procedure (45) for an
391 FDR of 5%. Significant genes are those with P-adj < 0.05 (Supplemental Table 8). ANOVA analysis was
392 then applied to the pan-ORFs to identify genes with significant variability of insertion counts across
393 strains. The normalized counts at each TA site for each gene were tabulated and averaged at the strain
394 level, excluding genes with mean < 20. Then one-way ANOVA was used to calculate the F-statistic and
395 P-value, adjusted for multiple testing as above.

396

397 **Genetic Interactions and Network Analysis:** A correlation analysis of mean transposon insertion counts
398 was performed for gene pairs across all *Mab* strains. Genes with significant variability by ANOVA (P-adj <
399 0.05) and insertion count < 20 or Z-max > 8 (used to filter out outliers) were selected, resulting in 751

varying genes. A Pearson correlation coefficient was calculated for gene pairs that were jointly present in at least 10 strains. This analysis identified 10,198 pairs of genes with a correlation of > 0.7 and adjusted p-value < 0.05. A network diagram based on these correlations was generated in Cytoscape v3.9.1 using the Edge-weighted Spring-embedded Layout.

To extract clusters of genes with similar TnSeq profiles, a network community analysis was performed based on a greedy algorithm. The degree of each gene was calculated, reflecting the number of genes correlated to it with cc > 0.7. The gene with the highest degree represented the most “central” gene in the network and was required to be present in at least 15 strains. We extracted the cluster of genes connected to the most central gene as the first cluster. To extract subsequent clusters, we identified the next most central gene whose neighbors did not overlap more than 20% with genes in previously selected clusters. The process was iterated until clusters contained fewer than 5 genes.

RNA Extraction and RT-PCR: For each strain, cultures were grown in biological triplicate to mid-log phase, diluted back in +/-500 ng/ml ATc, and grown for 18 hr to achieve target knockdown. Afterward, 2 OD_{600} equivalents of cells from each culture were harvested by centrifugation, resuspended in TRIzol (Thermo Fisher), and lysed by bead beating (Lysing Matrix B, MP Biomedicals). RNA extraction and subsequent RT-PCR experiments were performed as described by Akusobi et al. (27).

418 **References**

419 1. Baldwin SL, Larsen SE, Ordway D, Cassell G, Coler RN. The complexities and challenges of
420 preventing and treating nontuberculous mycobacterial diseases. PLoS Negl Trop Dis [Internet]. 2019
421 Feb 14 [cited 2020 May 3];13(2). Available from:
422 https://www.ncbi.nlm.nih.gov/pmc/articles/PMC6375572/

423 2. Adjemian J, Olivier KN, Seitz AE, Falkinham JO, Holland SM, Prevots DR. Spatial clusters of
424 nontuberculous mycobacterial lung disease in the United States. Am J Respir Crit Care Med. 2012
425 Sep 15;186(6):553–8.

426 3. Lee MR, Sheng WH, Hung CC, Yu CJ, Lee LN, Hsueh PR. Mycobacterium abscessus Complex
427 Infections in Humans. Emerg Infect Dis. 2015 Sep;21(9):1638–46.

428 4. Nessar R, Cambau E, Reyrat JM, Murray A, Gicquel B. Mycobacterium abscessus: a new antibiotic
429 nightmare. J Antimicrob Chemother. 2012 Apr;67(4):810–8.

430 5. Pang H, Li G, Wan L, Jiang Y, Liu H, Zhao X, et al. In vitro drug susceptibility of 40 international
431 reference rapidly growing mycobacteria to 20 antimicrobial agents. Int J Clin Exp Med.
432 2015;8(9):15423–31.

433 6. Nash KA, Brown-Elliott BA, Wallace RJ. A Novel Gene, erm(41), Confers Inducible Macrolide
434 Resistance to Clinical Isolates of Mycobacterium abscessus but Is Absent from Mycobacterium
435 chelonae. Antimicrob Agents Chemother. 2009 Apr;53(4):1367–76.

436 7. Hurst-Hess K, Rudra P, Ghosh P. Mycobacterium abscessus WhiB7 Regulates a Species-Specific
437 Repertoire of Genes To Confer Extreme Antibiotic Resistance. Antimicrob Agents Chemother
438 [Internet]. 2017 Nov 1 [cited 2020 May 27];61(11). Available from:
439 https://aac.asm.org/content/61/11/e01347-17

440 8. Koh WJ, Stout JE, Yew WW. Advances in the management of pulmonary disease due to
441 Mycobacterium abscessus complex. Int J Tuberc Lung Dis Off J Int Union Tuberc Lung Dis. 2014
442 Oct;18(10):1141–8.

443 9. Koh WJ, Jeong BH, Kim SY, Jeon K, Park KU, Jhun BW, et al. Mycobacterial Characteristics and
444 Treatment Outcomes in Mycobacterium abscessus Lung Disease. Clin Infect Dis Off Publ Infect Dis
445 Soc Am. 2017 Feb 1;64(3):309–16.

446 10. Tortoli E, Kohl TA, Brown-Elliott BA, Trovato A, Leão SC, Garcia MJ, et al. Emended description of
447 Mycobacterium abscessus, Mycobacterium abscessus subsp. abscessus and
448 Mycobacteriumabscessus subsp. bolletii and designation of Mycobacteriumabscessus subsp.
449 massiliense comb. Nov. Int J Syst Evol Microbiol. 2016 Nov;66(11):4471–9.

450 11. Bryant JM, Grogono DM, Rodriguez-Rincon D, Everall I, Brown KP, Moreno P, et al. Emergence and
451 spread of a human-transmissible multidrug-resistant nontuberculous mycobacterium. Science. 2016
452 Nov 11;354(6313):751–7.

453 12. Wee WY, Dutta A, Choo SW. Comparative genome analyses of mycobacteria give better insights into
454 their evolution. PLoS ONE [Internet]. 2017 Mar 14 [cited 2020 May 3];12(3). Available from:
455 https://www.ncbi.nlm.nih.gov/pmc/articles/PMC5349653/

456 13. Choo SW, Wee WY, Ngeow YF, Mitchell W, Tan JL, Wong GJ, et al. Genomic reconnaissance of
457 clinical isolates of emerging human pathogen Mycobacterium abscessus reveals high evolutionary
458 potential. Sci Rep. 2014 Feb 11;4(1):4061.

14. Ripoll F, Pasek S, Schenowitz C, Dossat C, Barbe V, Rottman M, et al. Non mycobacterial virulence genes in the genome of the emerging pathogen Mycobacterium abscessus. PloS One. 2009 Jun 19;4(6):e5660.

15. Gagneux S. Ecology and evolution of Mycobacterium tuberculosis. Nat Rev Microbiol. 2018;16(4):202–13.

16. Tan JL, Ng KP, Ong CS, Ngeow YF. Genomic Comparisons Reveal Microevolutionary Differences in Mycobacterium abscessus Subspecies. Front Microbiol [Internet]. 2017 [cited 2020 May 3];8. Available from: https://www.frontiersin.org/articles/10.3389/fmicb.2017.02042/full

17. Sapriel G, Konjek J, Orgeur M, Bouri L, Frézal L, Roux AL, et al. Genome-wide mosaicism within Mycobacterium abscessus: evolutionary and epidemiological implications. BMC Genomics. 2016 Feb 17;17:118.

18. Brockhurst MA, Harrison E, Hall JPJ, Richards T, McNally A, MacLean C. The Ecology and Evolution of Pangenomes. Curr Biol. 2019 Oct 21;29(20):R1094–103.

19. Rosconi F, Rudmann E, Li J, Surujon D, Anthony J, Frank M, et al. A bacterial pan-genome makes gene essentiality strain-dependent and evolvable. Nat Microbiol. 2022 Oct;7(10):1580–92.

20. Rousset F, Cabezas-Caballero J, Piastra-Facon F, Fernández-Rodríguez J, Clermont O, Denamur E, et al. The impact of genetic diversity on gene essentiality within the Escherichia coli species. Nat Microbiol. 2021 Mar;6(3):301–12.

21. Opijnen T van, Dedrick S, Bento J. Strain Dependent Genetic Networks for Antibiotic-Sensitivity in a Bacterial Pathogen with a Large Pan-Genome. PLOS Pathog. 2016 Sep 8;12(9):e1005869.

22. Coe KA, Lee W, Stone MC, Komazin-Meredith G, Meredith TC, Grad YH, et al. Multi-strain Tn-Seq reveals common daptomycin resistance determinants in Staphylococcus aureus. Peschel A, editor. PLOS Pathog. 2019 Nov 18;15(11):e1007862.

23. Karlinsey JE, Stepien TA, Mayho M, Singletary LA, Bingham-Ramos LK, Brehm MA, et al. Genome-wide Analysis of Salmonella enterica serovar Typhi in Humanized Mice Reveals Key Virulence Features. Cell Host Microbe. 2019 Sep 11;26(3):426-434.e6.

24. Allison F. Carey, Rock JM, Krieger IV, Chase MR, Fernandez-Suarez M, Gagneux S, et al. TnSeq of Mycobacterium tuberculosis clinical isolates reveals strain-specific antibiotic liabilities. PLOS Pathog. 2018 Mar 5;14(3):e1006939.

25. Rifat D, Chen L, Kreiswirth BN, Nuermberger EL. Genome-Wide Essentiality Analysis of Mycobacterium abscessus by Saturated Transposon Mutagenesis and Deep Sequencing. mBio. 2021 Jun 15;e0104921.

26. Foreman M, Gershoni M, Barkan D. A Simplified and Efficient Method for Himar-1 Transposon Sequencing in Bacteria, Demonstrated by Creation and Analysis of a Saturated Transposon-Mutant Library in Mycobacterium abscessus. mSystems [Internet]. 2020 Oct 27 [cited 2021 Mar 7];5(5). Available from: https://msystems.asm.org/content/5/5/e00976-20

27. Akusobi C, Benghomari BS, Zhu J, Wolf ID, Singhvi S, Dulberger CL, et al. Transposon mutagenesis in Mycobacterium abscessus identifies an essential penicillin-binding protein involved in septal peptidoglycan synthesis and antibiotic sensitivity. eLife. 2022 Jun 6;11:e71947.

498 28. Laencina L, Dubois V, Le Moigne V, Viljoen A, Majlessi L, Pritchard J, et al. Identification of genes
499 required for Mycobacterium abscessus growth in vivo with a prominent role of the ESX-4 locus. Proc
500 Natl Acad Sci U S A. 2018 30;115(5):E1002–11.

501 29. Jackman SD, Vandervalk BP, Mohamadi H, Chu J, Yeo S, Hammond SA, et al. ABySS 2.0:
502 resource-efficient assembly of large genomes using a Bloom filter. Genome Res. 2017
503 May;27(5):768–77.

504 30. Croucher NJ, Page AJ, Connor TR, Delaney AJ, Keane JA, Bentley SD, et al. Rapid phylogenetic
505 analysis of large samples of recombinant bacterial whole genome sequences using Gubbins. Nucleic
506 Acids Res. 2015 Feb 18;43(3):e15.

507 31. Goloboff PA, Farris JS, Nixon KC. TNT, a free program for phylogenetic analysis. Cladistics.
508 2008;24(5):774–86.

509 32. Ruis C, Bryant JM, Bell SC, Thomson R, Davidson RM, Hasan NA, et al. Dissemination of
510 Mycobacterium abscessus via global transmission networks. Nat Microbiol. 2021 Oct;6(10):1279–88.

511 33. Salazar AN, Abeel T. Approximate, simultaneous comparison of microbial genome architectures via
512 syntenic anchoring of quiver representations. Bioinformatics. 2018 Sep 1;34(17):i732–42.

513 34. Davidson RM. A Closer Look at the Genomic Variation of Geographically Diverse Mycobacterium
514 abscessus Clones That Cause Human Infection and Disease. Front Microbiol [Internet]. 2018 [cited
515 2020 May 3];9. Available from: https://www.frontiersin.org/articles/10.3389/fmicb.2018.02988/full#B15

516 35. DeJesus MA, Ambadipudi C, Baker R, Sassetti C, Ioerger TR. TRANSIT--A Software Tool for Himar1
517 TnSeq Analysis. PLoS Comput Biol. 2015 Oct;11(10):e1004401.

518 36. DeJesus MA, Gerrick ER, Xu W, Park SW, Long JE, Boutte CC, et al. Comprehensive Essentiality
519 Analysis of the Mycobacterium tuberculosis Genome via Saturating Transposon Mutagenesis. mBio.
520 2017 Jan 17;8(1):e02133-16.

521 37. Sullivan MR, McGowen K, Liu Q, Akusobi C, Young DC, Mayfield JA, et al. Biotin-dependent cell
522 envelope remodelling is required for Mycobacterium abscessus survival in lung infection. Nat
523 Microbiol. 2023 Jan 19;1–17.

524 38. Moore M, Frerichs JB. An unusual acid-fast infection of the knee with subcutaneous, abscess-like
525 lesions of the gluteal region; report of a case with a study of the organism, Mycobacterium
526 abscessus, n. sp. J Invest Dermatol. 1953 Feb;20(2):133–69.

527 39. Nakanaga K, Sekizuka T, Fukano H, Sakakibara Y, Takeuchi F, Wada S, et al. Discrimination of
528 Mycobacterium abscessus subsp. massiliense from Mycobacterium abscessus subsp. abscessus in
529 Clinical Isolates by Multiplex PCR. J Clin Microbiol. 2014 Jan;52(1):251–9.

530 40. Kurtz S, Phillippy A, Delcher AL, Smoot M, Shumway M, Antonescu C, et al. Versatile and open
531 software for comparing large genomes. Genome Biol. 2004;9.

532 41. Needleman SB, Wunsch CD. A general method applicable to the search for similarities in the amino
533 acid sequence of two proteins. J Mol Biol. 1970 Mar 28;48(3):443–53.

534 42. Brettin T, Davis JJ, Disz T, Edwards RA, Gerdes S, Olsen GJ, et al. RASTtk: a modular and
535 extensible implementation of the RAST algorithm for building custom annotation pipelines and
536 annotating batches of genomes. Sci Rep. 2015 Feb 10;5:8365.

537 43. Stamatakis A. RAxML version 8: a tool for phylogenetic analysis and post-analysis of large
538 phylogenies. Bioinformatics. 2014 May 1;30(9):1312–3.

539 44. Long JE, DeJesus M, Ward D, Baker RE, Ioerger T, Sassetti CM. Identifying essential genes in
540 Mycobacterium tuberculosis by global phenotypic profiling. Methods Mol Biol Clifton NJ.
541 2015;1279:79–95.

542 45. Benjamini Y, Hochberg Y. Controlling the False Discovery Rate: A Practical and Powerful Approach
543 to Multiple Testing. J R Stat Soc Ser B Methodol. 1995;57(1):289–300.

544

Figures and Legends

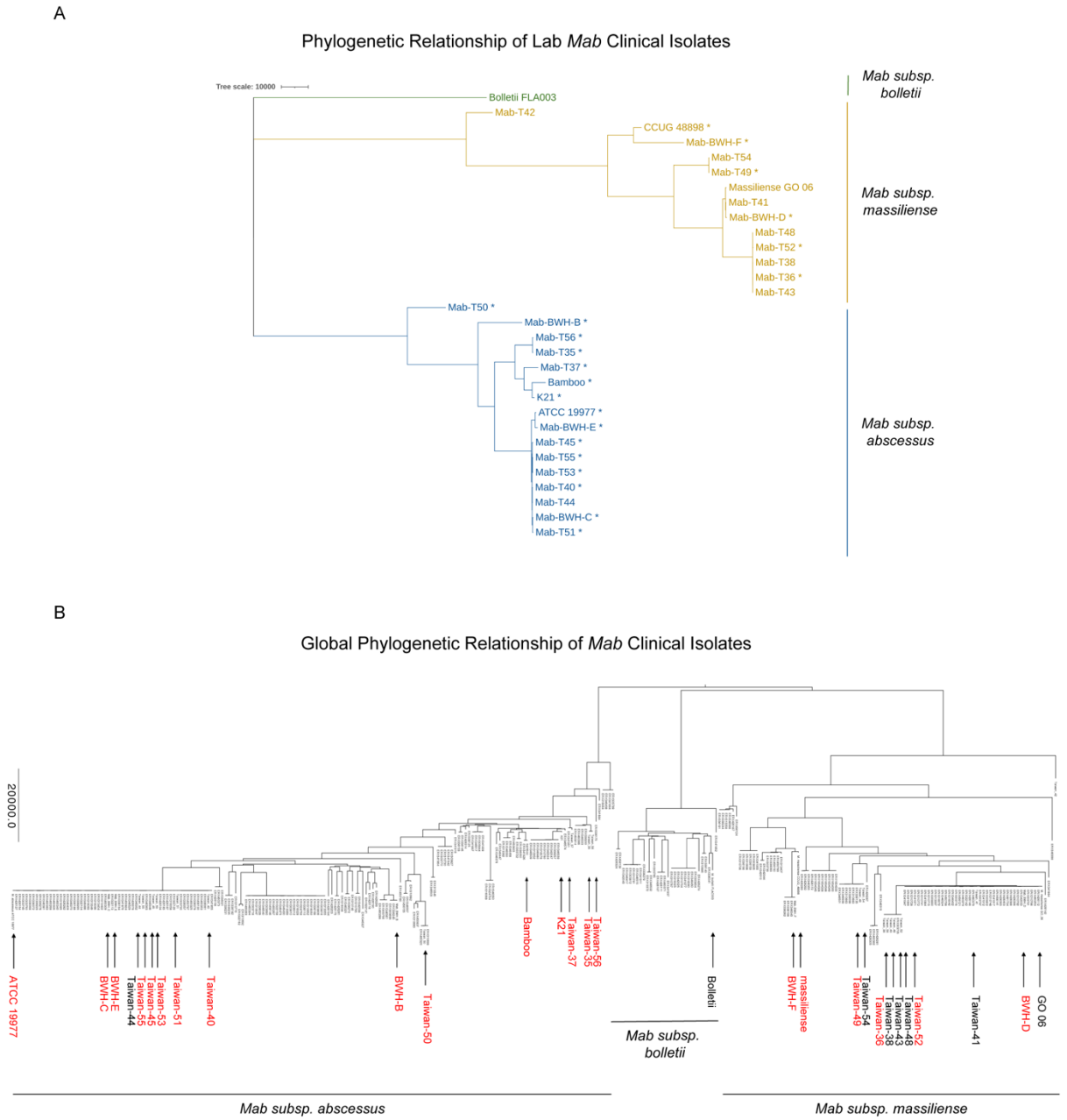

Figure 1: Phylogenetic Relationship of *Mab* Clinical Isolates. (A) Phylogenetic tree of 25 Mab clinical isolates and 5 reference strains. The tree is generated based on genome-wide SNPs, using Gubbins to filter out genomic regions potentially affected by recombination. Strains with transposon mutant libraries are marked with an '*' **(B)** Global phylogenetic tree of *Mab* clinical isolates using genomes of 307 clinical isolates from Bryant *et al.*, 2016. Strains in the lab are labeled with an arrow. Red arrows indicate strains that have transposon-mutant libraries.

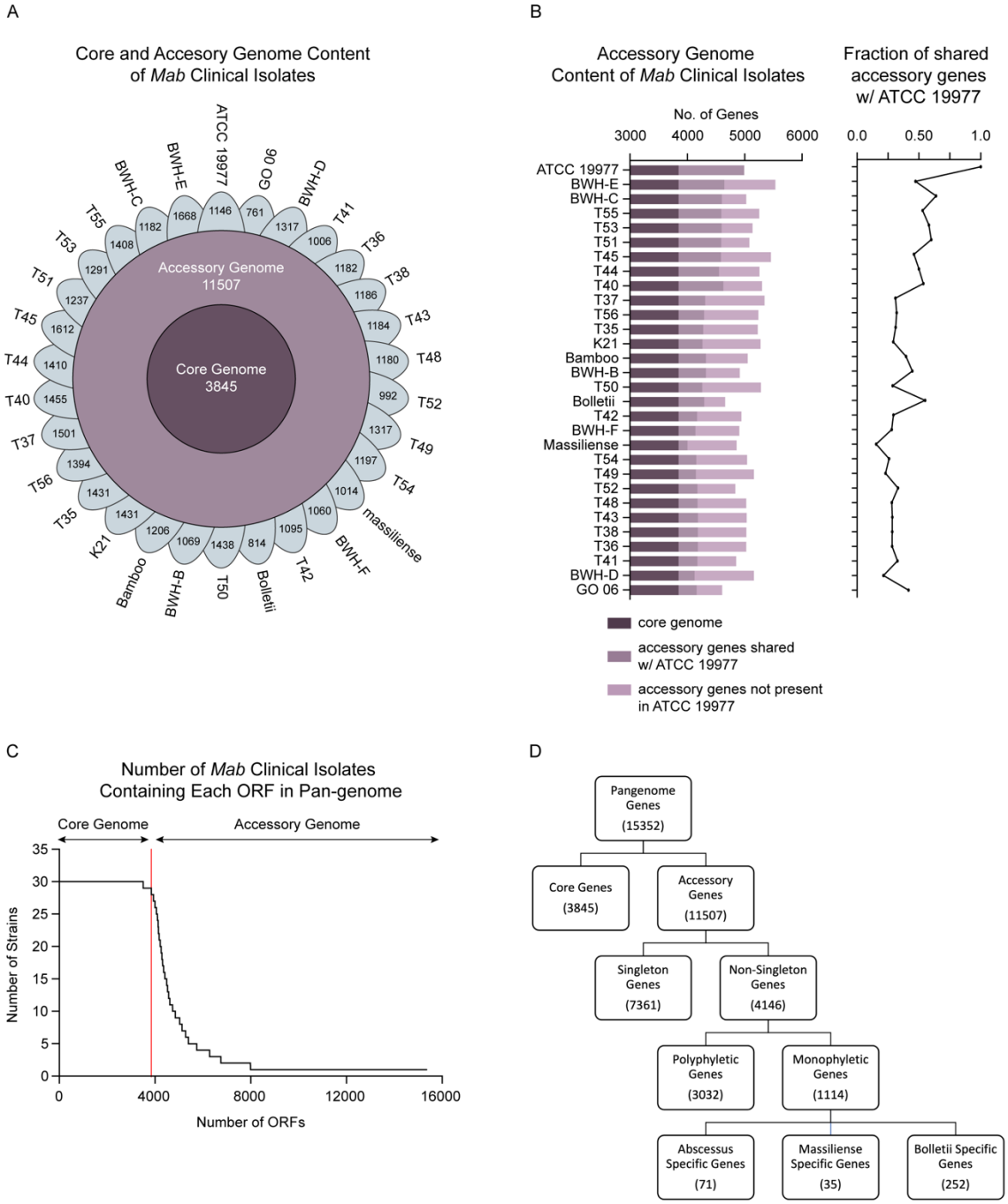

Figure 2: *Mab* has a large accessory genome. **(A)** Flower Pot diagram showing the breakdown of core and accessory genes in lab *Mab* clinical isolates. The outer leaflets represent the number of accessory genes in each clinical isolate. Strains are arranged counterclockwise based on the degree of similarity to the reference strain by core genome. **(B)** (*left*) Breakdown of accessory genome content in each clinical isolate. (*right*) Percentage of accessory gene content shared by the reference strain. **(C)** Number of ORFs present in the clinical isolates **(D)** Categorization of ORFs in the pan-genome.

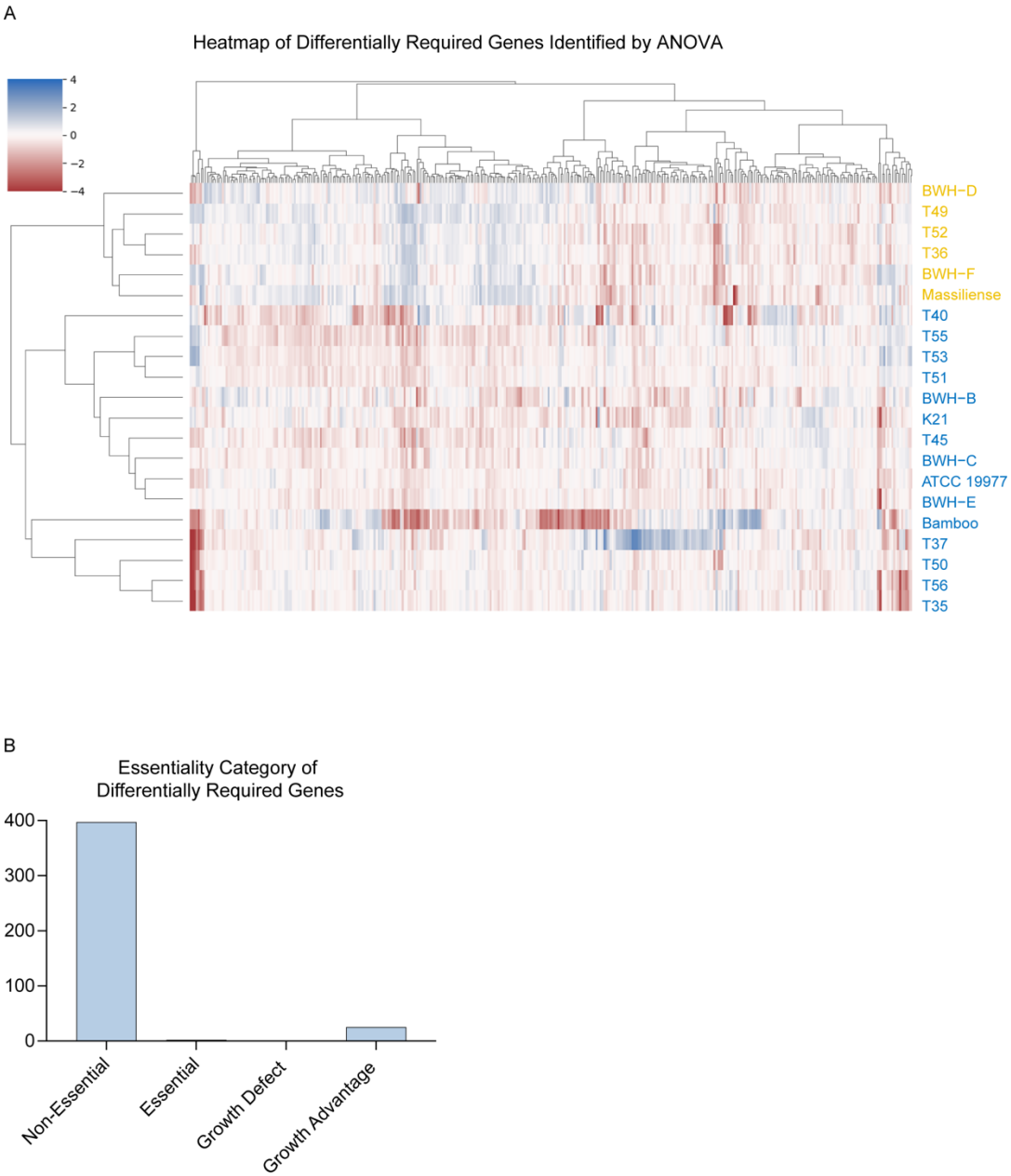

Figure 3: Summary of ANOVA results. (A) Heatmap depicting the log-2-fold-change (LFC) of insertion counts for the 425 differentially required genes in all isolates. **(B)** Essentiality category of the differentially essential genes in the ATCC 19977 reference strain.

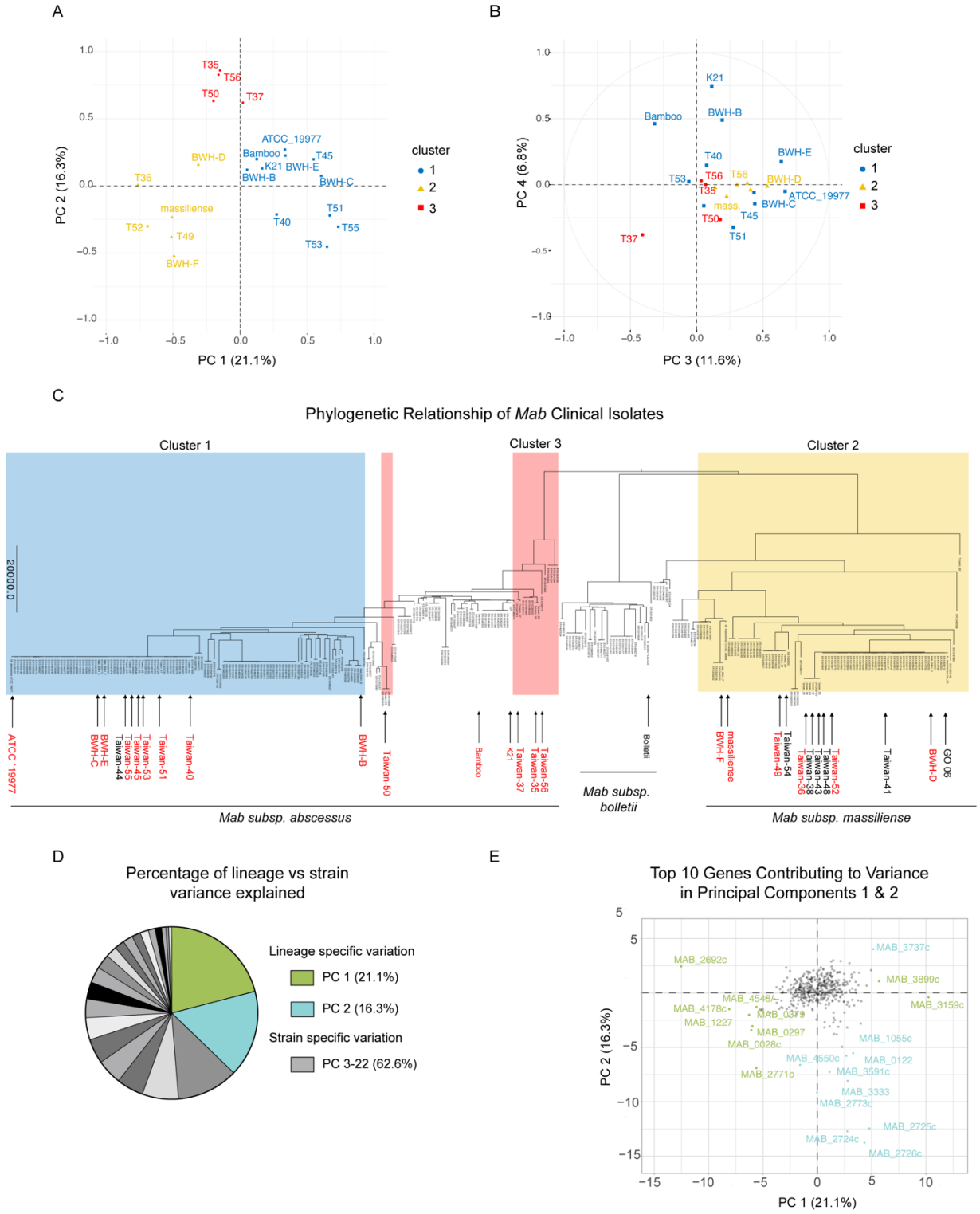

Figure 4: Principal Component Analysis of ANOVA Hits. (A) Principal components (PC) 1 & 2 of differentially required genes by ANOVA. **(B)** PC 3 & 4 **(C)** Phylogenetic tree of *Mab* clinical isolates shaded with rectangles highlighting clusters. **(D)** Percentage of variance explained by each of the principal components. **(E)** Plot depicting the top 10 contributing genes to the variance of PC 1 & 2.

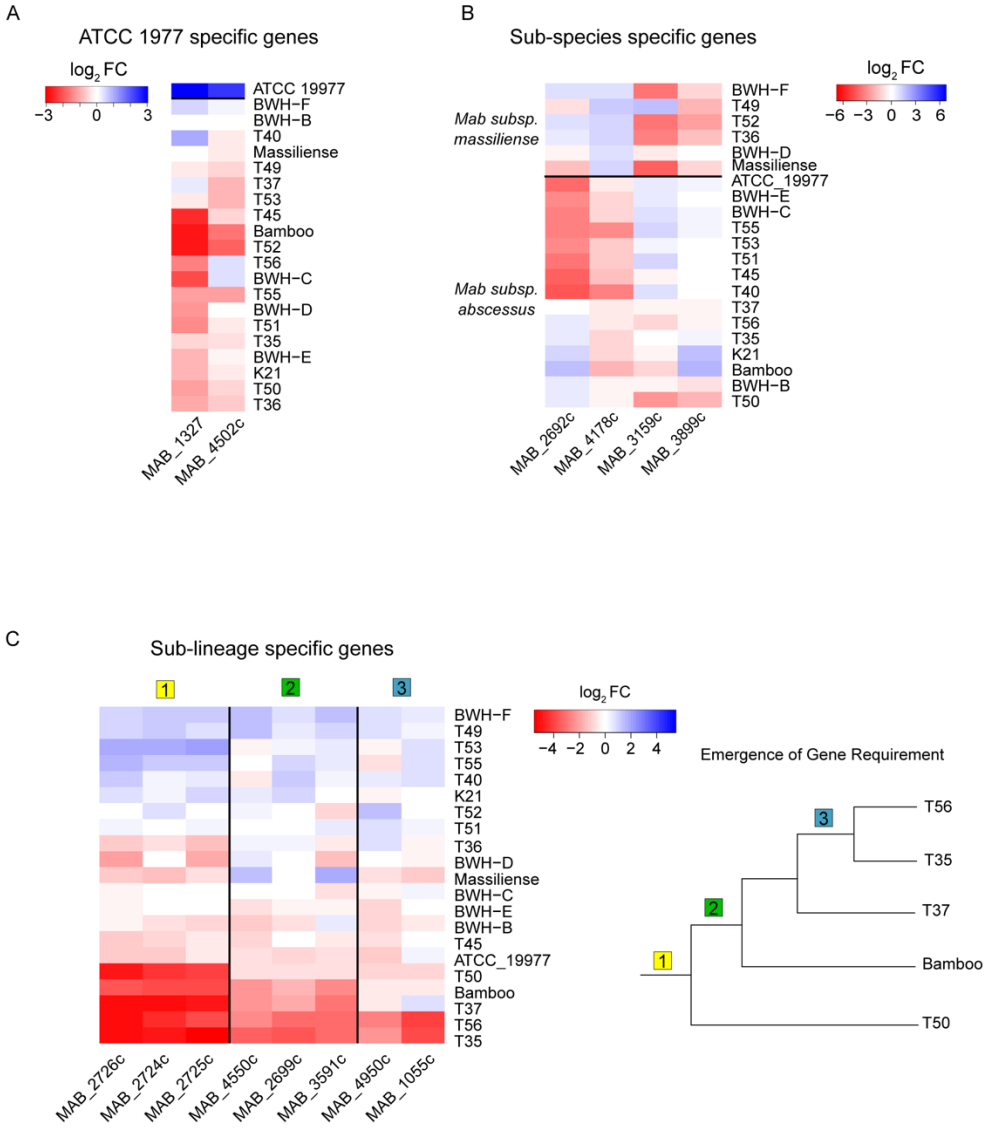

Figure 5: Sub-species and lineage-specific gene requirement (A) Genes specific to the reference ATCC 19977 strain **(B)** Subspecies-specific genes that separate *abscessus* and *massiliense* subspecies. **(C)** (*left*) Genes that are differentially required in cluster 1. (*right*) Schematized phylogenetic relationship of strains in cluster 1.

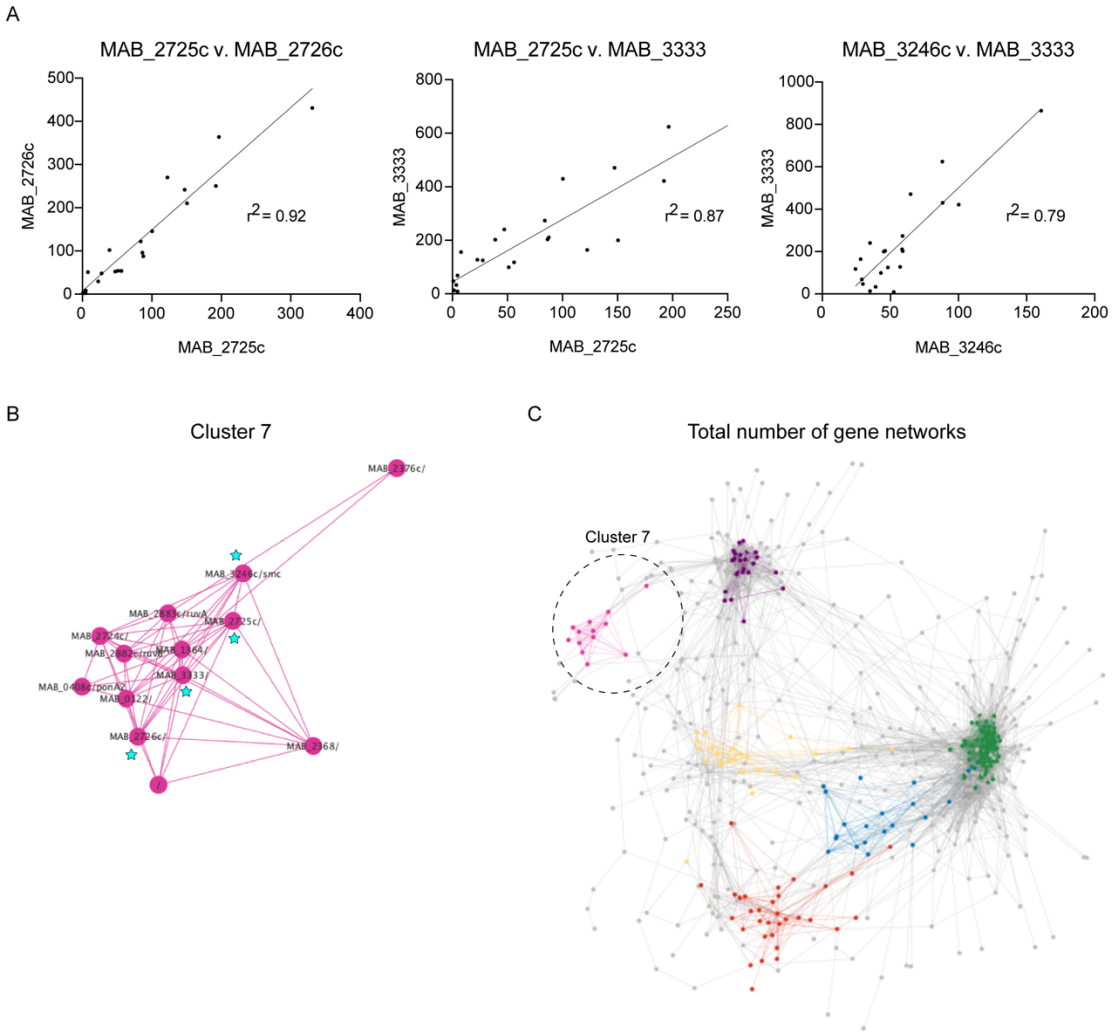

Figure 6: Network analysis of differentially required genes. (A) Correlation of transposon insertions between 3 gene pairs **(B)** Cluster 7 depicting 13 genes that are correlated with each other. Genes marked with blue stars are shown in panel A. **(C)** Network analysis depicting five additional clusters of 19 identified. Cluster 7 is highlighted by a dashed circle.

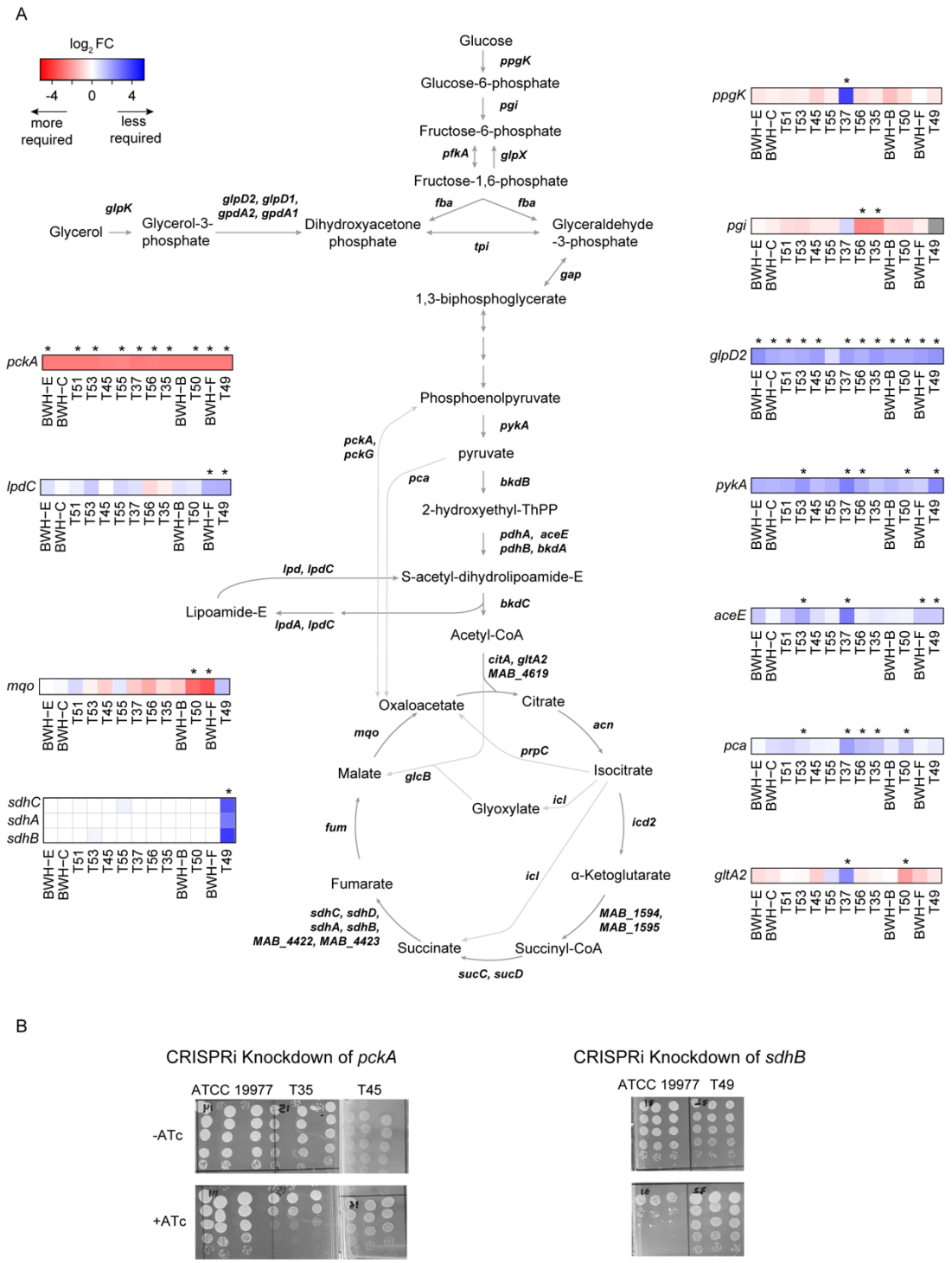

Figure 7: **Genetic requirement differences in carbon metabolism genes among clinical isolates. (A)** Schematic of genes in central carbon metabolism in *Mab*. All heatmaps showcase log-2-fold-change (LFC) relative to the reference strain. Genes with significant differences in LFC are highlighted with an "*" indicating a p-adj < 0.05. **(B)** CFU assay of *pckA* or *sdhB* clinical isolate knockdowns.

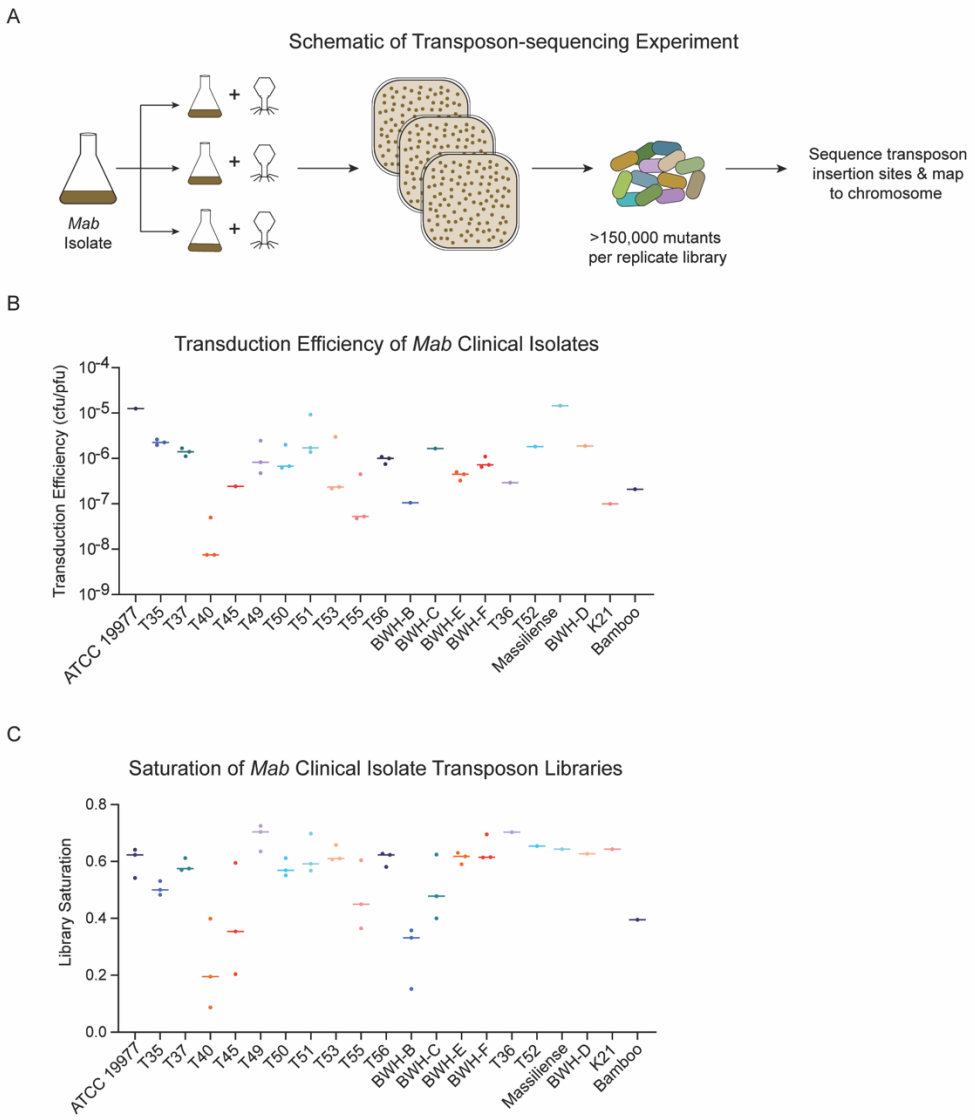

Supplemental Figure 1: Summary of TnSeq data. (A) Schematic of TnSeq experiment. **(B)** Transduction efficiency (CFU/PFU) of *Mab* clinical isolates. (**C)** Percent saturation of TnSeq libraries. The dotted line demarcates 30% library saturation used as a threshold for study inclusion.

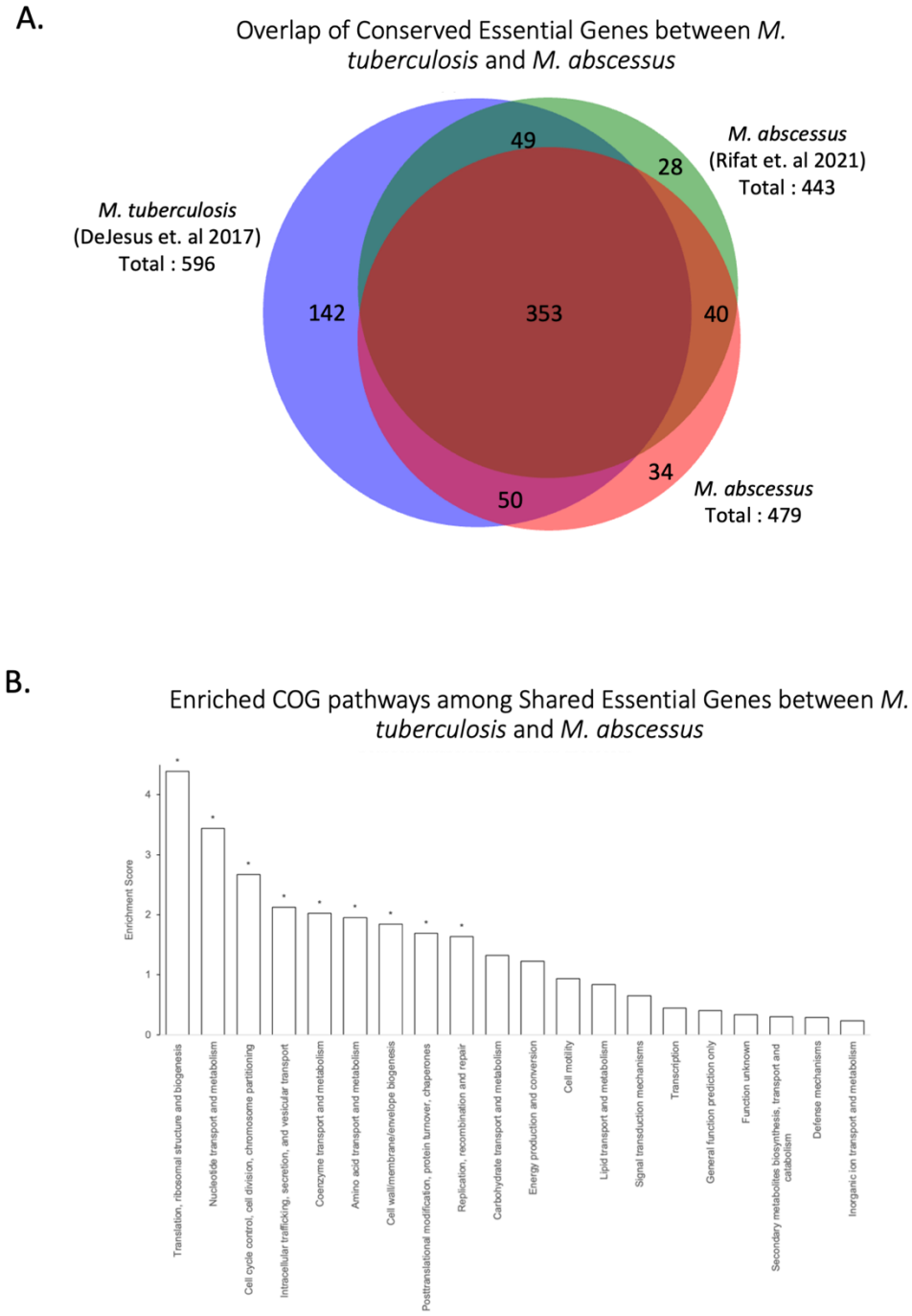

Supplemental Figure 2: Comparison of *M. tuberculosis* and *M. abscessus* essential genes. (A) Overlap of conserved essential genes between *Mtb* and *Mab.* **(B)** Enriched COG pathways of shared essential genes between *Mtb* and *Mab*. Pathways demarcated with an "*" indicate p-adj < 0.05.

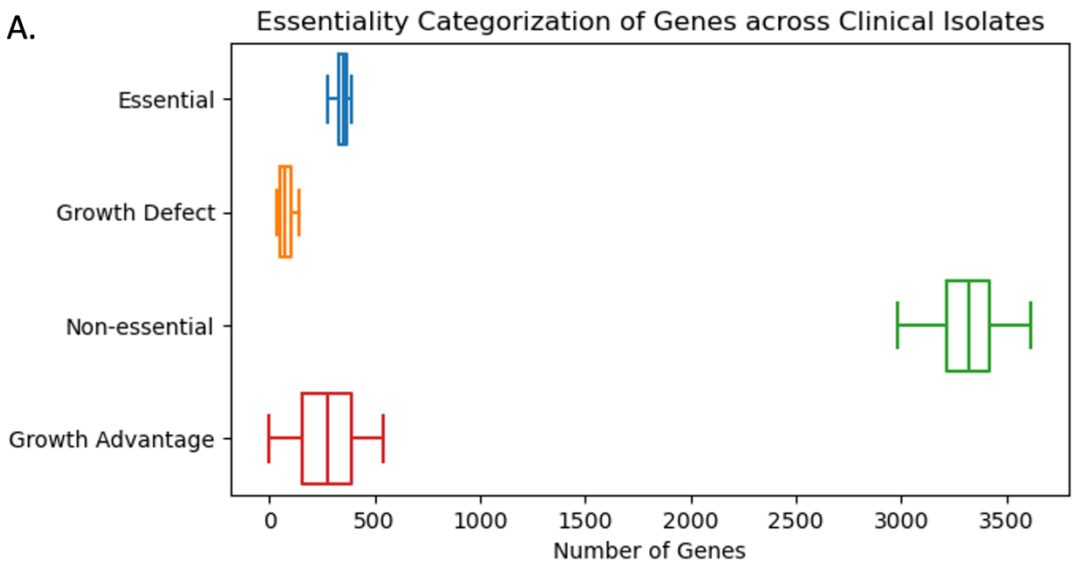

Supplemental Figure 3: Summary of gene essentiality category across *Mab* clinical isolates.

A.

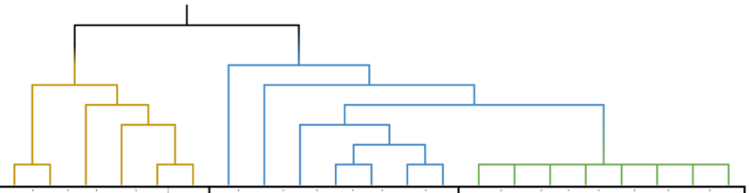

Orf	Description		CCUG 48898	BWH-F	T49	BWH-D	T36	T52	T50	BWH-B	T37	T56	T35	Bamboo	K21	ATCC 19977	BWH-E	T45	T55	T53	T40	BWH-C	T51
MAB_0189c	Probable arabinosyltransferase C	Massiliense Clade	GD	GD	GD	GD	GD	GD	GD	NE	NE	NE	NE*	NE	ES*	GD*	GD	NE	NE	GD*	NE	NE	GD
MAB_1124c	Probable para-aminobenzoate synthase component I		GD	GD	GD	GD	GD	GD	NE	NE*	NE	NE	NE	NE	NE	NE*	GD	NE*	NE*	NE*	NE*	NE*	GD
MAB_3159c	Probable malate:quinone oxidoreductase Mqo		ES	ES	NE	GD	GD	ES	GD	NE	NE	NE	NE	NE	NE	NE	NE	NE	NE	NE	NE	NE	NE
MAB_2897c	Conserved hypothetical protein (HIT family?)		GD	GD	GD*	GD*	GD*	GD	NE	GD	NE*	NE	NE	ES	NE	NE	NE	NE	NE	NE	NE	NE	NE
MAB_2896c	Probable phosphatidylinositol synthase PgsA		GD	GD	GD	GD	GD	GD	NE*	GD*	NE*	NE	NE	ES*	NE	NE	NE	NE*	NE*	NE*	NE*	NE	NE*
MAB_2895c	Putative acyltransferase		NE	NE	NE	ES	GD	ES	NE	GD*	NE	NE	NE	NE	NE	NE	NE	NE	NE	NE	NE	NE	NE
MAB_2725c	hypothetical protein	Abscessus Clade 1	NE	GA	GA	NE	NE	NE	GD	NE	GD	GD	GD	NE	NE	NE	NE	NE	GA	GA	NE	NE	NE
MAB_2726c	hypothetical protein		NE	GA	GA	NE	NE	NE	GD	NE	GD	GD	GD	NE	NE	NE	NE	NE	GA	GA	NE	NE	NE
MAB_2724c	hypothetical protein		NE	GA	GA	NE	NE	NE*	GD	NE	GD	GD	GD	NE	NE	NE	NE	NE	GA	GA	NE	NE	NE
MAB_2699c	Probable pseudouridine synthase RluD		NE	NE	NE	NE	NE	NE	NE	NE*	GD	GD	GD	NE	NE	NE	NE	NE	NE	NE	NE	NE	NE
MAB_2692c	hypothetical protein	Abscessus Clade 2	NE	NE	NE*	NE	NE	NE	NE	NE*	NE	NE	NE	NE	NE	GD	GD	ES	GD	ES*	ES	GD	GD
MAB_1682	Probable NAD-dependent epimerase/dehydratase		NE	NE	NE	NE	NE	NE	GD*	NE	NE	NE	NE	ES*	NE	GD*	GD*	GD	ES*	GD	ES	GD	NE*
MAB_2298	Dephospho-CoA kinase		NE	NE	NE	NE	NE	NE	NE	NE	NE	NE	NE	NE	NE	GD	NE	GD	GD	NE*	GD	NE	NE*
MAB_1692	Putative polyketide synthase Pks16/acyl-CoA synthetase		NE	GD	NE	NE	NE	NE	NE	NE	NE	NE	NE*	NE*	GD	NE*	GD	GD	GD	NE	GD	GD	GD
MAB_0210	hypothetical protein		U	U	U	U	U	U	NE*	U	GD*	NE	NE	NE	NE	ES	NE	ES	ES	ES	ES	ES	ES
MAB_3963c	hypothetical protein		NE	GD*	NE	NE	NE	NE*	NE	GD	NE	NE	NE	NE	NE	NE	GD*	GD	GD	GD	NE*	NE*	GD
MAB_3655c	Probable glycerol-3-phosphate dehydrogenase		NE	NE*	NE	NE	NE	NE	NE	NE*	NE	NE	NE	NE	NE	GD	NE	NE*	GD	NE*	NE*	NE	GD

Supplemental Figure 4: Analysis of shared essential genes in *Mab* clinical isolates. Analysis of clade-specific essentials in *Mab* clinical isolates. The HMM calls of the clade-specific genes across all 21 *Mab* isolates (ignoring genes with low-confidence calls, marked with an asterisk). The phylogeny of the 21 isolates is depicted above with the *massiliense* clade (includes all *massiliense* isolates) in yellow, the *abscessus* clade 1 in blue, and *abscessus* clade 2 in green. The highlighted gray genes are seen in Figure 5, depicting lineage-specific gene essentiality.

A

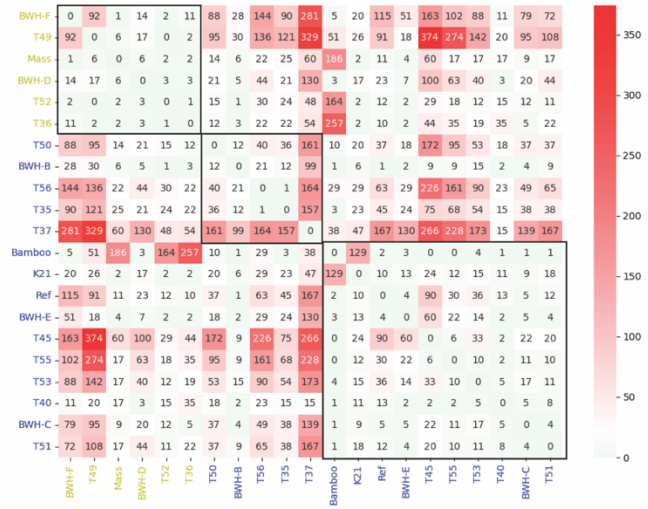

Supplemental Figure 5: Pairwise Resampling Heatmap Matrix. Each number in comparison represents the differentially required genes between two clinical isolates. Top left corner represents subsp. *massiliense* – *massiliense* comparisons. Bottom right comparisons represent subsp. *abscessus* – *abscessus* comparisons with strains more closely related to the ATCC 19977 reference strain.

612

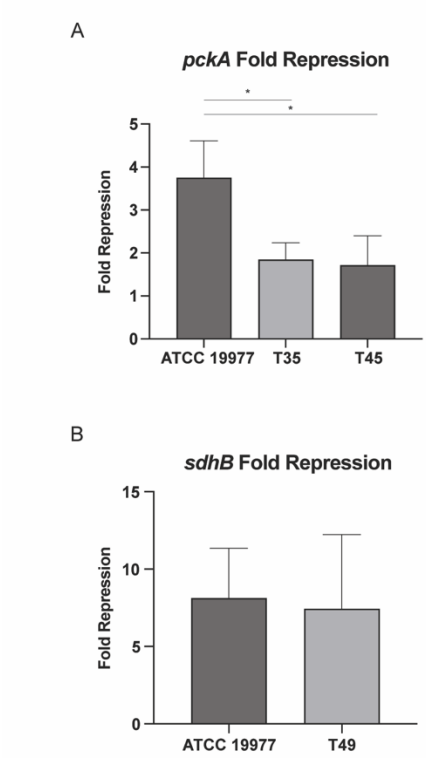

613
614
615
616 **Supplemental Figure 6: Fold Repression of *pckA* and *sdhB.* (A).** Fold repression of *pckA* as
617 measured by RT-qPCR. "*" signifies $p < 0.05$ by student's t-test. **(B)** Fold repression of *sdhB* as measured
618 by RT-qPCR.